

Heat Transfer Enhancement in a Duct with Two Right Angled Bends

Dr. Jalal M. Jalil*, Dr. Talib K. Murtadha** & Sanaa T. Mousa***

Received on: 28/7/2009

Accepted on: 11/3/2010

Abstract

A numerical study was carried out to predict the behavior of complex flow and forced convection heat transfer characteristics in a duct with two right-angled bends for both laminar and turbulent flows. The finite differences method was employed to solve the Navier – Stokes and energy equations. The thermal boundary conditions at the duct walls are adopted by using an isothermal for laminar flow and transient heat conducted with convection for turbulent flow. The equations of vorticity and energy have been solved by using the explicit method. The computations were performed for step height ratios ($H/W=2, 3, \text{ and } 4$), inlet air velocities ($0.12\text{-}1.0 \text{ m/s}$) for Reynolds number ($568\text{-}33334$), ambient air temperature of ($30\text{-}35^\circ\text{C}$), duct wall thickness of ($0.002\text{-}0.004 \text{ m}$) and different duct metal on the behavior of the flow and heat transfer. Generally, the effect of the step ratio on the bulk temperature and local heat transfer is minor for H/W equal or greater than 3 . Also, it is found that both flow and heat transfer patterns change drastically from laminar to turbulent flows. Moreover, in the turbulent flow regime, the maximum heat transfer rates occur at increasing of the inlet air velocity and the ambient air temperature, also at decrease in the duct width and wall thickness with aluminum duct. Also, it was found that the bulk temperature tends to reach a higher value at the duct bends (separation and recirculation regions) and lower values for the local Nusselt number. The numerical results of local Nusselt number along the duct wall for laminar flow were compared with published experiment results. The comparison indicates reasonable agreement.

دراسة عددية لانتقال الحرارة للجريان الطبقي والمضطرب في مجرى هوائي ذي انحناءتين قائمتين

الخلاصة

تم في هذا البحث إجراء دراسة عددية للتكهن بسلوك الجريان المعقد وخصائص انتقال الحرارة بالحمل القسري للجريان الطبقي والاضطرابي داخل مجرى هوائي ذي انحناءتين قائمتين. استخدمت في هذه الدراسة طريقة الفروق المحددة (Finite Differences Method) لحل معادلات نافير - ستوكس (Navier-Stokes) والطاقة ثنائيًا البعد (2-D). كذلك تم اعتماد الشروط الحدية الحرارية ذات درجة حرارة ثابتة (Isothermal) لجدران المجرى الهوائي عند الجريان الطبقي وذات توصيل حراري انتقالي للجريان الاضطرابي. إن الحلول العددية للمعادلات الحاكمة فقد أنجزت باستخدام طريقة التراخي (Relaxation) لحل معادلة دالة الانسياب. إما معادلات الدوامية و الطاقة فقد تم حلها باستخدام الطريقة العددية البينية (Explicit). لقد أجريت الدراسة لنسب ارتفاع الخطوة ($2, 3, 4$) كذلك تم دراسة تأثير اختلاف سرع دخول للهواء من (0.12m/s) إلى (1.0m/s) لأرقام رينولد تتراوح من ($568\text{-}33334$) لدرجات حرارة للهواء المحيط (30°C و 35°C) و سمك الجدار (0.002m و 0.004m) مع اختلاف معدن

*Electromechanical Engineering Department, University of Technology/Baghdad

**Mechanical Engineering Department, University of Technology/Baghdad

***Ministry of Transportation /Baghdad

المجرى الهوائي على سلوك الجريان و انتقال الحرارة. بشكل عام وجد ان تأثير نسبة ارتفاع الخطوة إذا كانت اكبر أو تساوي (3) يكون ثانويًا على كل من درجة الحرارة الظاهرية و على انتقال الحرارة الموضعي. كذلك تبين ان نماذج الجريان و انتقال الحرارة تتغير تغيرًا شديدًا من الجريان الطبقي إلى الجريان الاضطرابي. فضلًا عن ذلك فان أعلى معدلات انتقال الحرارة في الجريان الاضطرابي تحدث عند زيادة كل من سرعة الهواء الداخل ودرجة حرارة الهواء المحيط و كذلك عند تقليل كل من عرض المجرى و سمك جدار المجرى ذي معدن الألمنيوم. كما وجدت الدراسة ان الدرجة الحرارية الظاهرية تميل للوصول إلى أعلى قيمة عند انحناءات المجرى (مناطق الانفصال و إعادة الدوران) بينما يكون العكس لعدد نسلت الموضعي. وعند مقارنة النتائج العددية للدراسة الحالية مع النتائج العملية المنشورة، فقد بينت المقارنة تطابقًا مقبولًا.

Nomenclature

$C_{\mu}, C_{1\epsilon}, C_{2\epsilon}$	Constants in turbulence model	—
C_v	Specific heat of duct metal at 20°C	J/kg.°C
E	Energy content of volume element	—
H	Step height	m
ke	Thermal conductivity of the duct metal	W/m.K
k	Turbulent kinetic energy	m ² /s ²
Nu	Local Nusselt number	—
Q	Heat transfer rate	W
Re	Reynolds Number	—
T_b	Bulk temperature	°C
T_w	Wall temperature	°C
T_o	Ambient temperature	°C
t	Time	s
u, v	Velocity components in x and y directions	m/s
U_{in}	Velocity of inlet air	m/s
$V_{element}$	Volume	m ³
x, y	Cartesian coordinates	m

Greek Symbols

ϵ	Dissipation rate of turbulent kinetic energy	m ³ /kg.s
ρ_m	Density of duct metal	kg/m ³
σ_t	Turbulent coefficient	—
$\sigma_k, \sigma_\epsilon$	Coefficients for k, ϵ	—
μ	Dynamic viscosity of air	N.s/m ²
ν	Kinematics viscosity of air	m ² /s
ν_t	Eddy or turbulent viscosity	m ² /s
ν_e	Effective kinematics viscosity	m ² /s
Γ_e	Effective diffusion coefficient ,	m ² /s
ψ	Stream function	m ² /s
ξ	Vorticity	1/s
ϕ	General dependent variable	—
S_ϕ	Source term	—
Δt	Time step	—

Introduction

The accurate prediction of heat transfer rates is essential in the design of air duct or thermal system. Due to continuing demands on engineers to develop smaller, more efficient air conditioning systems, forced flow separation has been utilized as a mechanism to enhance convective heat transfer. Also, the need for more efficient air ducts or heat exchange devices has led to the development of a variety of unconventional internal flow passages to enhance the heat-transfer coefficient. One such passage is the non-straight duct, or the corrugated-wall channel. Corrugated ducts such as duct with two right angled bends are often used as a passage for the purpose of heat transfer enhancement, in which flows are perpendicular to the corrugations and move in undulating path as they encounters the successive peaks and valleys. Also, the flow in a duct, which has steps or sharp bends, is often seen in many actual engineering applications, such as passages of air conditioning systems, components of fluid machinery, diffusers, etc [1, 2].

Izumi, R., Oyakawa, K., Kaga, S., and Yamashita, H., 1981 [3] measured experimentally the local heat transfer rates along the wall of channel which has two right-angled bends. Amano, R, S., 1984 [4] reported a numerical study on the flow and heat transfer in the channel with two right -angled bends. He investigated numerically the behavior of the flow and heat transfer for step ratios, $H/W = 1, 2$ and 3 and for Reynolds number ranging from $200 - 2000$. Collier, B. D., 2000 [5]

developed the 2-D modeling of a diffuser with 30° angle.

Chakravarthy, S., Bose, T.K., Batten, P., Palaniswamy, S., Goldberg, U., and Perroomian, O., 2000 [6] presented a study on the flow through an internal square passage containing a 180° U-bend. The tube walls are heated to represent the internal walls of a turbine- blade-cooling passage. The flow was observed to separate around the 90° section and reattach approximately two diameters downstream the bend exit.

It can be seen from the literature review that there are different methods for analyzing the fluid flow and heat transfer accomplished by using non straight ducts or channels; However emphasis was on a duct or channel with a corrugated wall or duct which had steps or bends which induce turbulent complex flow phenomena such as separation at bend corners, flow reattachment, and flow recirculation and subsequently may have a profound influence on the heat transfer results. In the present study, full Navier – Stokes and energy equations are replaced in laminar and turbulent flows by stream function and vorticity $\psi-\xi$ based on the finite difference numerical solution using an explicit scheme which was used to simulate the fluid flow and heat transfer in duct with two right angled bends. Also, the behavior of the complex flow, the distribution of temperature, the effects of duct walls material and thickness used in heat conduction wall boundary, the bulk temperature, or energy average fluid temperature across the duct, and local Nusselt number variation along the walls duct are investigated for different step ratios $H/W=2, 3$ and 4 , for different ambient temperatures,

duct material, and for different inlet air velocities.

2-Theory

2-1 The Problem Description

The study of heat transfer by forced convection is focused on the fluid flow in a duct with two right-angled bends shown in Figure 1. The fluid is considered incompressible unsteady with 2-D and constant properties.

2-2 Governing Equations, [7, 8, 9, 10, 11]

The stream-function / vorticity method has some attractive features. The pressure makes no appearance, and, instead of dealing with the continuity equation and two momentum equations, there is the need to solve only two equations to obtain the stream function and the vorticity. Some of the boundary conditions can be rather easily specified: when an external irrotational flow lies adjacent to the calculation domain, the boundary vorticity can conveniently be set equal to zero. However, there are some major disadvantages to the stream – function / vorticity method. The value of vorticity at a wall is difficult to specify and it may cause trouble in getting a converged solution.

The stream function is defined by

$$u = \frac{\partial \psi}{\partial y} \quad \dots (1)$$

$$v = -\frac{\partial \psi}{\partial x} \quad \dots (2)$$

The Navier Stokes equations in term of Stream vorticity are:

$$\frac{\partial^2 \psi}{\partial x^2} + \frac{\partial^2 \psi}{\partial y^2} = -\chi \quad \dots (3)$$

$$\frac{\partial \xi}{\partial t} + \frac{\partial \psi}{\partial y} \frac{\partial \xi}{\partial x} - \frac{\partial \psi}{\partial x} \frac{\partial \xi}{\partial y} = \nu \left(\frac{\partial^2 \xi}{\partial x^2} + \frac{\partial^2 \xi}{\partial y^2} \right) \quad \dots (4)$$

$$\frac{\partial T}{\partial t} + \frac{\partial \psi}{\partial y} \frac{\partial T}{\partial x} - \frac{\partial \psi}{\partial x} \frac{\partial T}{\partial y} = \Gamma \left(\frac{\partial^2 T}{\partial x^2} + \frac{\partial^2 T}{\partial y^2} \right) \quad \dots (5)$$

$$\Gamma = \frac{\nu}{\sigma}$$

Turbulent Model (k-ε):

$$\frac{\partial k}{\partial t} + \frac{\partial y}{\partial y} \frac{\partial k}{\partial x} - \frac{\partial y}{\partial x} \frac{\partial k}{\partial y} = \frac{n_r}{s_k} \left(\frac{\partial^2 k}{\partial x^2} + \frac{\partial^2 k}{\partial y^2} \right) + n_t \left[2 \left(\frac{\partial^2 \psi}{\partial x \partial y} \right)^2 + 2 \left(\frac{\partial^2 \psi}{\partial x \partial y} \right)^2 + \left(\frac{\partial^2 \psi}{\partial y^2} - \frac{\partial^2 \psi}{\partial x^2} \right)^2 \right] - e \quad \dots (6)$$

$$\frac{\partial e}{\partial t} + \frac{\partial y}{\partial y} \frac{\partial e}{\partial x} - \frac{\partial y}{\partial x} \frac{\partial e}{\partial y} = \frac{n_r}{s_e} \left(\frac{\partial^2 e}{\partial x^2} + \frac{\partial^2 e}{\partial y^2} \right) + C_{2e} \frac{e}{k} \left[2 \left(\frac{\partial^2 \psi}{\partial x \partial y} \right)^2 + 2 \left(\frac{\partial^2 \psi}{\partial x \partial y} \right)^2 + \left(\frac{\partial^2 \psi}{\partial y^2} - \frac{\partial^2 \psi}{\partial x^2} \right)^2 \right] - C_{2e} \frac{e^2}{k} \quad \dots (7)$$

2-3 General Form of the Governing (PDES)

The general form of the transport equations for stream function ψ, vorticity ξ turbulent scales k, ε and temperature T all has the form [12,13].

$$\frac{\partial}{\partial t} (f) + \frac{\partial y}{\partial y} \frac{\partial f}{\partial x} - \frac{\partial y}{\partial x} \frac{\partial f}{\partial y} = \frac{\partial}{\partial x} \left(df \frac{\partial f}{\partial x} \right) + \frac{\partial}{\partial y} \left(df \frac{\partial f}{\partial y} \right) + S_f \quad \dots (8)$$

Where the terms on left sides are convection terms and the terms on the right side are diffusion and source terms. The source term S_f in the governing Equation 8 is given in Tables (1, 2), where (G) is the generation term which is given as:

$$G = n_t \left[2 \left(\frac{\partial^2 \psi}{\partial x \partial y} \right)^2 + 2 \left(\frac{\partial^2 \psi}{\partial x \partial y} \right)^2 + \left(\frac{\partial^2 \psi}{\partial y^2} - \frac{\partial^2 \psi}{\partial x^2} \right)^2 \right]$$

$$\Gamma_k = \frac{n_t}{s_k}$$

$$\Gamma_e = \frac{n_t}{S_e}$$

2-4 Initial and Boundary Conditions

In order to begin the computations, some initial conditions have to be set at time (t=0.0). These initial conditions are specified at all grid points for dimensional variables in laminar and turbulent flows. In this study, the solution is highly dependent on these initial conditions. For the laminar flow the initial conditions are:

$$\xi = 0.0, T = T_{in} = 21^\circ C$$

For the turbulent flow the initial conditions are defined as:

$$\xi = k = \epsilon = 0.0, T = T_{in}$$

The wall vorticity of Woods [7] is:

$$\xi_\omega = \frac{3(\psi_\omega - \psi_{\omega+1})}{\Delta n^2} - \frac{1}{2}\xi_{\omega+1} \dots (9)$$

The boundary conditions are shown clearly in Figures 2 and 3.

2-5 Relaxation Method

Under-relaxation is a very useful device for nonlinear problems. It is often employed, also in the present study, to avoid divergence in the iterative solution of strongly nonlinear equation 3. Equation 3 is derived, in which the central finite difference approximations have been introduced:

$$\frac{Y_{(m+1,n)}^{-2Y_{(m,n)} + Y_{(m-1,n)}}}{\Delta x^2} + \frac{Y_{(m,n+1)}^{-2Y_{(m,n)} + Y_{(m,n-1)}}}{\Delta y^2} + x(m,n) = error = 0 \dots (10)$$

The equation (10) is solved by substituting in the current values of ψ and ξ where upon the right- hand side error will be non zero. In order to solve the equation, the error has to be subtracted from both sides. Thus, if a small change $\Delta\psi_{(m,n)}$ is made to the

center point value $\psi_{(m,n)}$ to do this, the following equation is obtained:

$$\left(\frac{-2}{\Delta x^2} - \frac{2}{\Delta y^2} \right) \Delta\psi_{(m,n)} = -Error \dots (11)$$

Or

$$\Delta\psi_{(m,n)} = \frac{Error}{2 \cdot \left(\frac{1}{\Delta x^2} + \frac{1}{\Delta y^2} \right)} \dots (12)$$

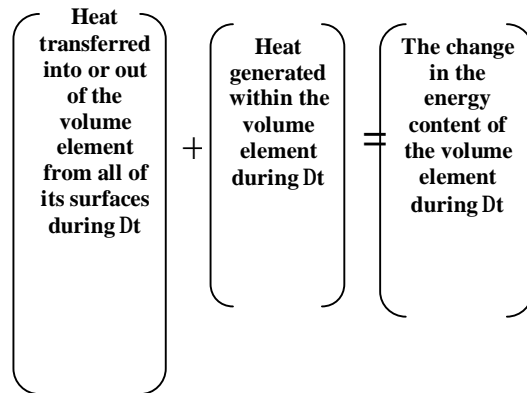
$\psi_{(IT+1)}$ can then be calculated from $\psi_{(IT)}$ from the previous iteration as:

$$Y_{(IT+1)} = Y_{(IT)} + RF \cdot \Delta Y_{(m,n)} \dots (13)$$

Where (RF) is the relaxation factor.

2-6 Transient Heat Conduction on the Wall

In the transient problems, the temperatures change with time as well as position, the finite difference solution requires discretization in time in addition to discretization in space. This can be done by selecting a suitable time step Δt and solving for the unknown nodal temperatures



repeating for each Δt until the solution at the desired time is obtained [14, 15]. Choosing a small Δt will increase the accuracy of the solution, but it will increase the computation time. In this study, the energy balance on volume element during a time interval

Δt that is considered from boundary conditions ABCD and EFGH can be expressed as:

$$\Delta t \sum_{\text{All sides}} Q + \Delta t \dot{G}_{\text{element}} = \Delta E_{\text{element}} \dots\dots(14)$$

Where the rate of heat transfers Q normally consists of conduction terms and involves convection for boundary nodes. Noting that:

$$\Delta E_{\text{element}} = M C_v \Delta T = \rho_m V_{\text{element}} C_v \Delta T \text{ where:}$$

Because, non heat is generated within the volume element during Δt therefore, \dot{G}_{element} is equal zero.

Dividing Equation 10 by Δt gives:

$$\sum_{\text{allsides}} Q = \frac{\Delta E_{\text{element}}}{\Delta t} = r_m V_{\text{element}} C_v \frac{\Delta T}{\Delta t} \dots\dots (15)$$

$$\sum_{\text{allsides}} Q = r_m V_{\text{element}} C_v \frac{T_{(m,n)}^{i+1} - T_{(m,n)}^i}{\Delta t} \dots\dots (16)$$

It appears that the time derivative is expressed in forward difference form in the explicit method. In this study, consider a rectangular duct wall in which heat condition and convection are significant in the x- and y- directions, and consider a unit depth of $\Delta z=1$ in the z-direction. Now divide the x or y- thick plane of the duct wall into a rectangular mesh of nodal points spaced Δx or Δy and thick a part in the x- and y- directions, and consider a general boundary node (m, n). The network of grid point has two distance coordinate x and y, as independent variable, and the spacing of the grid lines is uniform in the x and y directions. The grid points is employed for the computation were 177 x 46, 177 x 61, and 177 x 76 for step ratios H/W = 2, 3, and 4 respectively. These numbers of meshes are reached after optimization to have stable solution.

3- Discussion

3-1 Results of Laminar Flow

Figure 4 shows the flow field by stream function for different step ratios and for $U_{in}=0.14$ m/s. For the flow of H/W=2, the separated flow at the corner B reattaches on the CD walls. Consequently, a recirculating region is formed near the concave corner C. This feature is represented by a peak stream function values near the corner C, but it is represented by the negative velocity profile on the BC wall. Meanwhile, the separated flow at the corner B in this duct of H/W=3 and 4 has reattachments on the wall BC, thus creating two recirculating regions on the BC wall. The flow also separates at corner G and reattaches on the wall GH in every H/W case, thus causing a recirculating region beyond the corner G on this wall. At the cross section of the first bend B, there is a similar trend in stream function contours for all step ratios.

Temperature contours for $T_w=35^\circ\text{C}$ and $U_{in}=0.14$ m/s with different step ratios are given in Figure 5. This figure illustrates larger temperature contour deformation near the walls BC and near the wall GH as the H/W=2 than as the H/W=3 and 4. But, for H/W=4 the temperature values are larger than that for H/W=2 and 3 near the walls and near the concave corner C and F near the corners B and G. This behavior of thermal field is due to transfer of thermal energy from the hot wall with hot high stream velocity to the air far from the wall and to the low stream velocity which has less temperature. Also, the temperature distribution in H/W=2 has higher consideration difference than in H/W=3 and 4

because the flow reaches faster the section DH due to the small step ratio and small duct length.

Local Nusselt numbers were computed along the duct walls to investigate the local heat transfer characteristics affected by these duct. The accuracy of the present theory, as well as the numerical technique was verified by studying the uniform wall temperature and transient heat conduction in laminar and turbulent flows respectively of forced convection from a duct with two-right angled bends and comparing laminar results with the experimental data found in the literature. The computed local Nusselt numbers along the duct walls in the present study are compared with the experimental data obtained by Izumi et al. [6] for step ratio $H/W=3$ and for $Re=300$ in Figure 6. The agreement is relatively good in the inlet and the redeveloping flow regions for AB and EF walls but a discrepancy is observed near the corners B, C, F, and G. While the computed results show minimum values at B, F, and at the position one duct width from the corners C and G, the experimental data do not show this trend clearly. The heat transfer rates must be minimum in recirculating regions at these positions. These discrepancies may be in the experimental wake or due to error. The heat conduction effect through the duct metal is not computed in the present numerical study.

3-2 Results of Turbulent Flow

Figure 7 show the predicted distribution of the turbulent flow field by stream function for different step ratios, $U_{in}=0.5$ m/s, and for ambient

temperature $T_o=40^\circ\text{C}$ with wall thickness (0.0007m). For the flow of $H/W=2$, flow separated at the corner B and reattaches on the wall CD, thus creating a recirculating flow along the wall BC. This feature is represented by peak stream function values near the concave corner C, also by a peak velocity at the corner B and the negative velocity on the wall BC. Also, these figures illustrate the separated flow at the corner B in the duct of ($H/W=3$ and 4) reattaches on the BC wall, thus creating two recirculating regions on the wall BC. This feature is represented by the negative velocity profile near the concave corner C. The separated flow at the corner B will also cause a flow deflection toward the opposite side of this duct walls. The flow also separates at the corner G and reattaches on the wall GH in every H/W case, thus causing a recirculating region beyond the corner G on this wall. As a result the stream function values reach it's their lower at the position closer to the corner G, but the velocity reaches its peak. At the cross section of the first bend, B, there is a similar trend in stream lines and velocity profile for all step ratios.

Figure 8 shows the temperature distribution for ($H/W=2, 3$ and 4), $U_{in}=0.5$ m/s, wall thickness (0.0007m) and ambient temperature ($T_o=40^\circ\text{C}$). It can be seen that the transfer of thermal energy towards the main stream is increased with increasing step ratio due to increase in the interchange of stream function and vorticity between the wall and separated flow with main stream at high step ratio.

Figure 9 shows the variation in mean air bulk temperature along the

duct for different step ratios, for ($U_{in}=0.5\text{m/s}$ and $T_o=40^\circ\text{C}$). This figure illustrates an increase in mean air bulk temperature at duct exit and it increases sharply from the first and second bends, also increasing the step ratios gives the higher air bulk temperature variation along the duct, as seen for the $H/W=4$ with respect to the $H/W=2$ and 3. This is due to enhancing heat transfer between duct walls and air in duct, also between separating flow and main flow, caused by increasing step ratios. Figure 10 illustrates an increase in mean air bulk temperature at bends and exit of this duct for different inlet air velocity, $T_o=40^\circ\text{C}$ and $H/W=3$ with thickness (0.0007m), also increasing the inlet air velocity value gives higher air bulk temperature variation along the duct, as seen in the ($U_{in}=1.0\text{m/s}$) flow. This is due to increasing the transfer of thermal energy at the position of the cornering flow or reversed corner flow at the higher inlet air velocity ($U_n=1.0\text{m/s}$).

Local Nusselt numbers were computed along the duct walls to investigate the local heat transfer characteristics affected by the duct bends. Figure 11 shows the behavior of the local Nusselt number (Nu) distribution along the upper and lower duct walls for the different step ratios, $T_o=40^\circ\text{C}$, $U_{in}=0.5\text{m/s}$ and wall thickness (0.0007m). For every step ratio, the (Nu) number begins with higher values at A due to the cooler duct wall and air at the entrance region of the duct and then reduces from A to the corner B, also, the (Nu) number decreases sharply from the corner B due to hotter air therefore the flow separates and it remains shortly at a nearly constant value up

to the concave corner C where the (Nu) number becomes minimum due to a reversed corner flow will cause heated air. The (Nu) number, then, increases to its peak value at about a half duct width to the right of the corner C because of the flow impingement from upstream. The distribution also shows another peak in (Nu) number at about one and a half duct width down stream from the corner C attributed to the flow deflection promoted by the hotter air at the corner G.

For $H/W=3$ and 4 the pattern of the (Nu) number distribution is the same as that for $H/W=2$ except that the distributions along the BC wall for $H/W=2$ are more distinguishable than for $H/W=3$ and 4. Also the (Nu) number decreases with increasing step ratio. At the same time, the (Nu) number distribution for the EFGH wall is the same as that for ABCD wall except that the (Nu) number decreases sharply from the start E to the concave corner G and the (Nu) number increases at duct exit for increasing step ratio.

Figure 12 shows the effect of wall thickness of the duct on the (Nu) Number distributions at the duct walls, it is clear that increasing thickness will increase the values of (Nu) number for upper and lower duct walls at end duct, as seen for thickness (0.004m) with respect to the thickness (0.0007m and 0.002m). This is due to lowest heat transfer from ambient temperature to the duct walls and then to the air flow in duct.

Figure 13 shows higher (Nu) number values at the upper and Lower walls of duct made of iron metal (Fe) when compared with aluminum metal duct (Al) but the

same thickness (0.002m and $H/W=3$) is used. This figure illustrates that Al-metal will enhance heat transfer from both ambient and separation flow to the main air stream in the duct, because the value of thermal conducting for Al-metal is higher the Fe-metal. Also, in each case we can see similar trends in the distribution of local (Nu) numbers.

Conclusions

- 1- The flow patterns and temperature distribution for laminar and turbulent flows are strongly affected by the two bends, the step ratio, inlet air velocity, wall temperature of this duct. The heat transfer characteristics are correlated effectively.
- 2- The effect of the step ratio on the flow behavior and temperature pattern for laminar and turbulent flows are the same for H/W larger than or equal to 3.
- 3- Increasing the inlet air velocity of the laminar and turbulent flows for all step ratios will increase the flow separation at the first bend, which causes larger deflection of flow towards the opposite side of this duct wall. Also, the recirculating regions beyond the second bend on this wall will increase.
- 4- The effect of step ratio on the bulk temperature T_b and Nusselt number (Nu) is minor for H/W larger than or equal to 3 for laminar and turbulent flows. In general, increasing step ratio will increase the duct length, which causes a higher rate of heat transfer and then higher values of T_b at duct exit.

5- Increasing of duct width W of this duct for turbulent flow will increase the recirculating region and decrease the heat transfer rate which causes lower T_b values than when W is smaller, thus these bends often are used in large duct systems. Also, they are simpler than curvature duct.

6- Decreasing of the wall thickness, and increasing of the T_o for $H/W=3$ will increase the heat transfer rates between the ambient air and interior fluid in this duct. This causes higher T_b values, but (Nu) values will decrease for small thickness, and they are the same for increasing T_o .

7- The aluminum metal of the duct walls will increase the heat transfer rates, which causes the higher T_b values than for iron metal. Also, the iron metal is in expensive, thus often is used in ducting design.

References

- [1] Streeter, V. L., "Hand book of fluid dynamics", McGraw Hill, New York, 1961.
- [2] Bradshaw, P., "Turbulence", Topics in Applied Physics, Vol.12, Springer-Verlage Berlin Heidelberg, 1976.
- [3] Izumi, R., Oyakawa, K., Kaga, S., and Yamashita, H., "Fluid Flow and Heat Transfer in Corrugated wall channels", JSME J. Vol. 47, No. 416, pp. 657- 665, 1981.
- [4] Amano, R. S., "Laminar Heat Transfer in a Channel With Two Right - Angled Bends" ASME J. of Heat Transfer, Vol. 106, No.3, pp. 591 - 596, 1984.

- [5] Collier, B. D., "Vortex Model for Control of Differ Pressure Recovery", Technical Note: Dscl 00 – 05, Technical paper, 2000.
- [6] Chakravarthy, S., Bose, T.K., Batten, P., Palaniswamy, S., Goldberg, U., and Peroomian, O., "Convective Heat Transfer Inside Rotating Tubes", AIAA paper 2000 – 3356.
- [7] Roache, P. J., "Computational Fluid Dynamics", Hermosa, Albuquerque, New Mexico, 1982.
- [8] Fox, R. W., Mc Donald, A.T., "Introduction to Fluid Mechanics", 5ed, John Wiley, New York, 2000.
- [9] Rohsenow, W.M., Hartnett, J.P. and Ganic, E.N. "Heat Transfer Fundamentals", McGraw – Hill, New York, 1985.
- [10] Iatridis, M.L., "A Theoretical Study of Buoyancy Driven Circulation in a Liquid Drop", M.Sc. thesis, University of Liverpool, 1987.
- [11] Cebeci, T., and Bradshaw, P. "Momentum Transfer in Boundary Layers", Hemisphere, Washington, 1977.
- [12] Morsi, Y. S. M., and Clayton, B. R. "Determination of Principal Characteristics of Turbulent Swirling Flow along Annuli", Int. J. Heat & Fluid Flow, Vol.7, S No.3, September 1986.
- [13] Patankar, S.V. "Numerical Heat Transfer and Fluid Flow", McGraw Hill, New York, 1980.
- [14] Cengel, Y.A. "Heat Transfer", International Edition, McGraw–Hill, 1998.
- [15] Arpact, V.S., "Conduction Heat Transfer", Addison – Wesley, 1966.

Table (1) Empirical Constants in the k- e model

C_m	S_K	S_e	C_{1e}	C_{2e}	S_t
0.09	1.00	1.30	1.44	1.92	1.00

Table (2) source terms in Equation 8

Equation	f	df	Sf
Stream function	y	1	x
Vorticity	x	ne	0.0
Temperature	T	G_e	0.0
Kinetic energy	k	G_k	G-e
Dissipation rate	e	Ge	$C_{1e} \frac{e}{K} G - C_{2e} \frac{e^2}{K}$

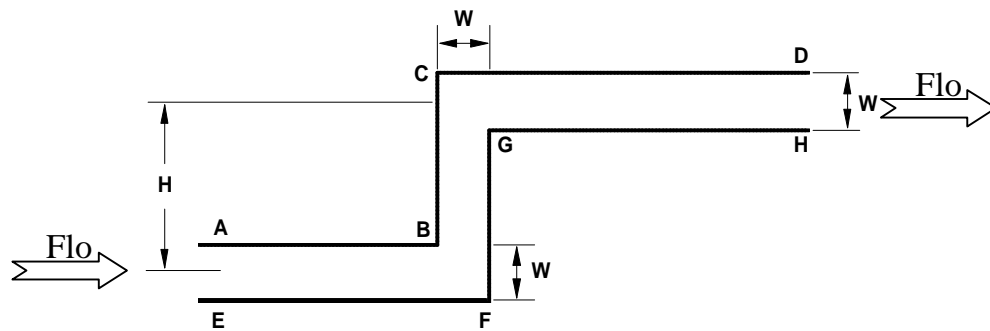


Figure (1) Typical flow domain (H/W=3).

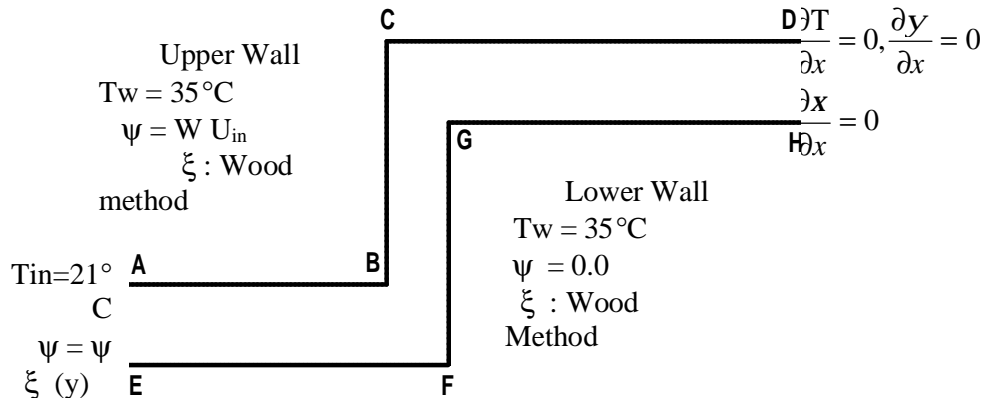


Figure (2) Boundary conditions for laminar flow at $H/W=3$.

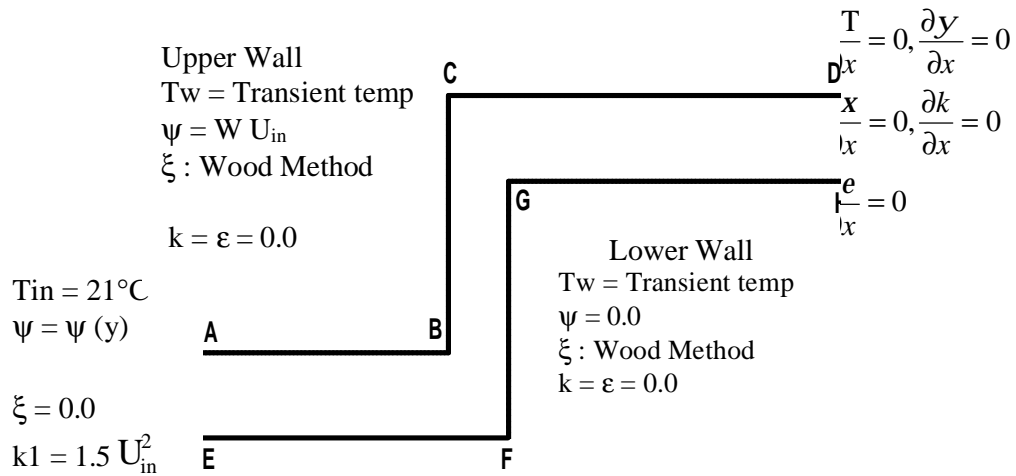
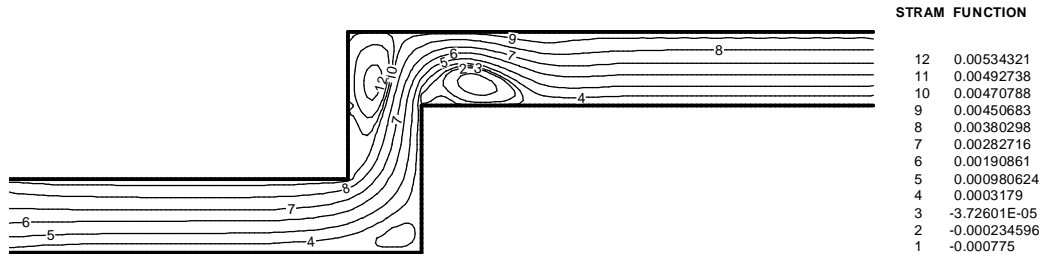
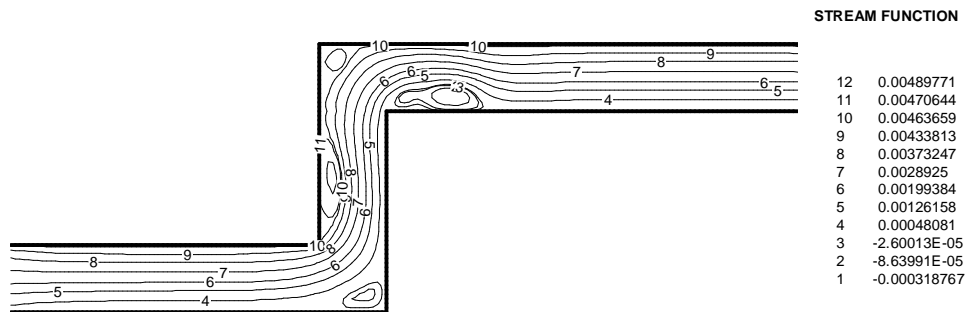


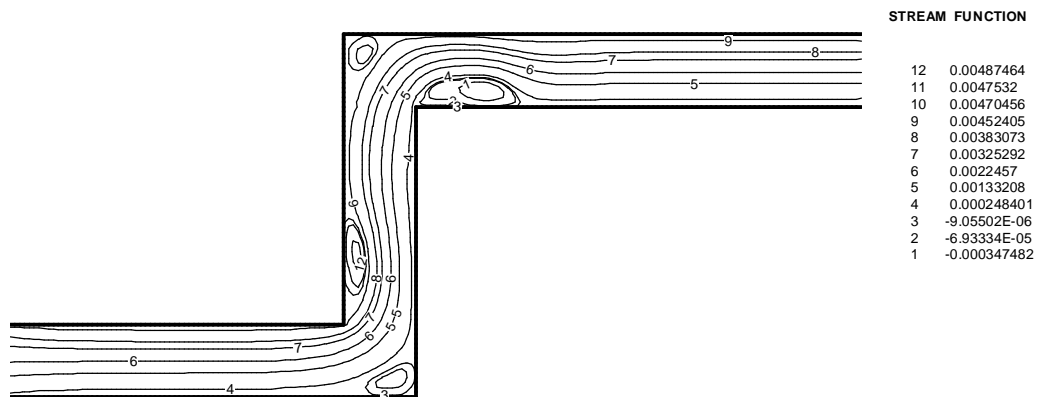
Figure (3) Boundary conditions for turbulent flow at $H/W=3$.



(a) $H/W=2$, $U_{in}=0.14$ m/s, $T_w=35^\circ\text{C}$

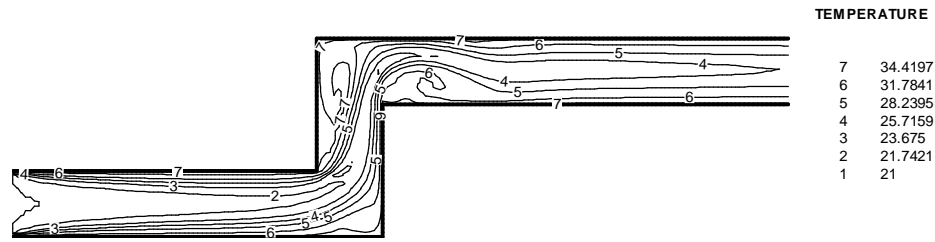


(b) $H/W=3$, $U_{in}=0.14$ m/s, $T_w=35^\circ\text{C}$

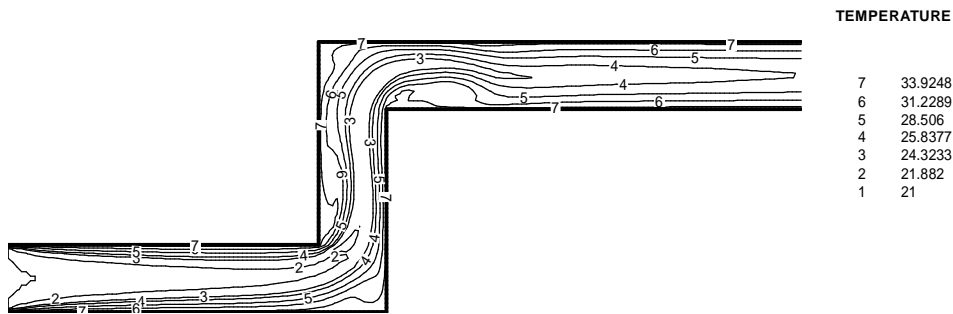


(c) $H/W=4$, $U_{in}=0.14$ m/s, $T_w=35^\circ\text{C}$

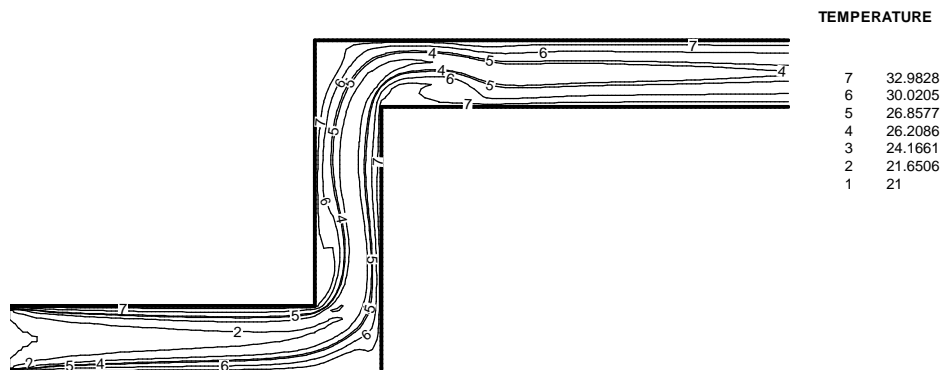
Figure 4 Contours of stream function for laminar flow, (a- $H/W=2$, b- $H/W=3$, and c- $H/W=4$), for $U_{in}=0.14$ m/s, and $T_w=35^\circ\text{C}$.



(a) $H/W=2$, $U_{in}=0.14$ m/s, $T_w=35^\circ\text{C}$



(b) $H/W=3$, $U_{in}=0.14$ m/s, $T_w=35^\circ\text{C}$



(c) $H/W=4$, $U_{in}=0.14$ m/s, $T_w=35^\circ\text{C}$

Figure (5) Contours of temperature for laminar flow, (a- $H/W=2$, b- $H/W=3$, and c- $H/W=4$), $U_{in}=0.14$ m/s, and for constant wall temperature $T_w=35^\circ\text{C}$.

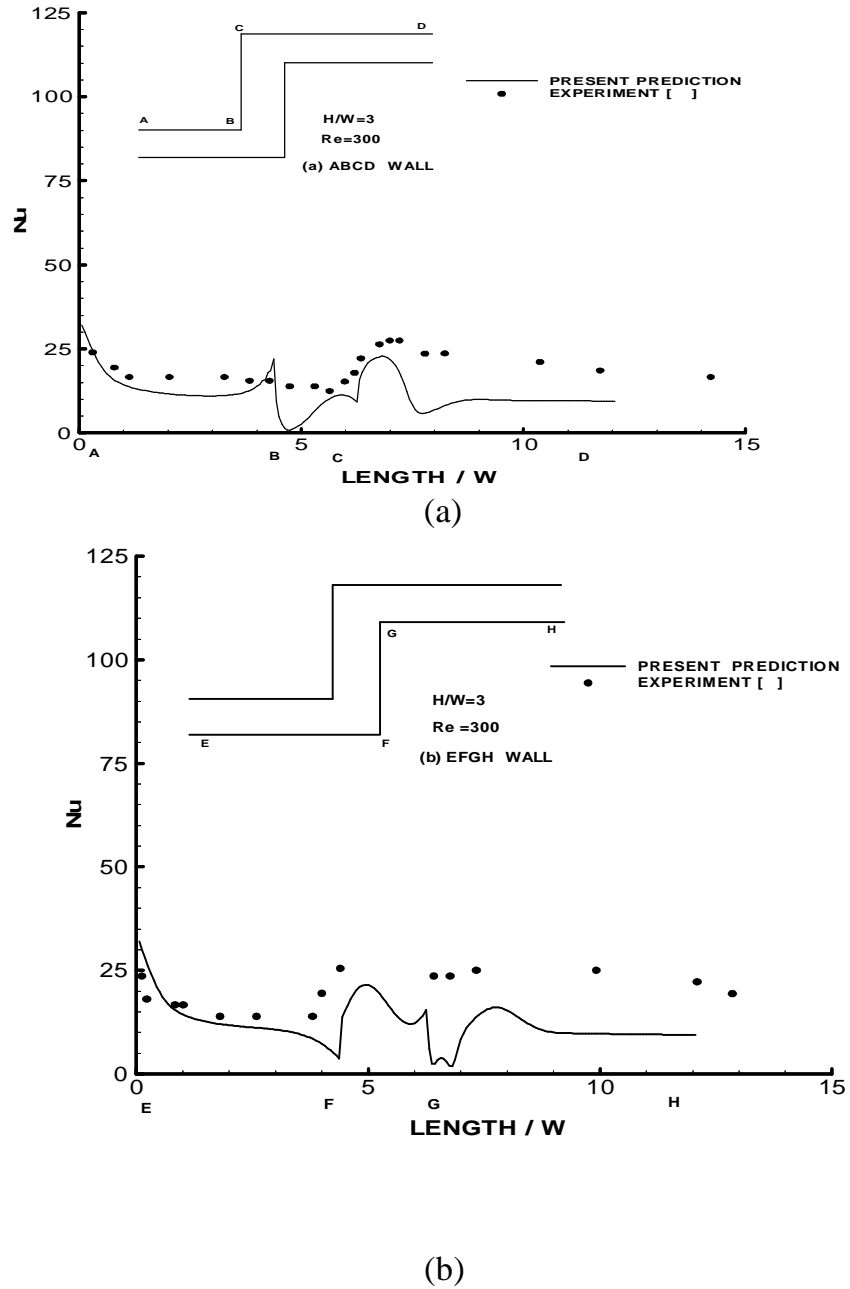
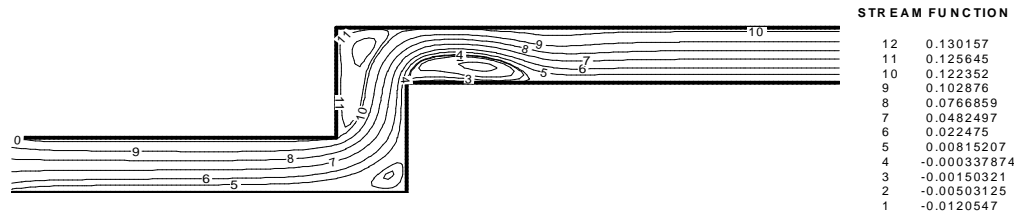
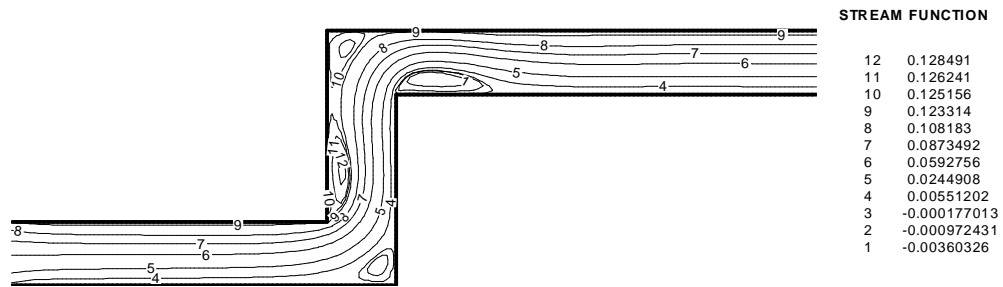


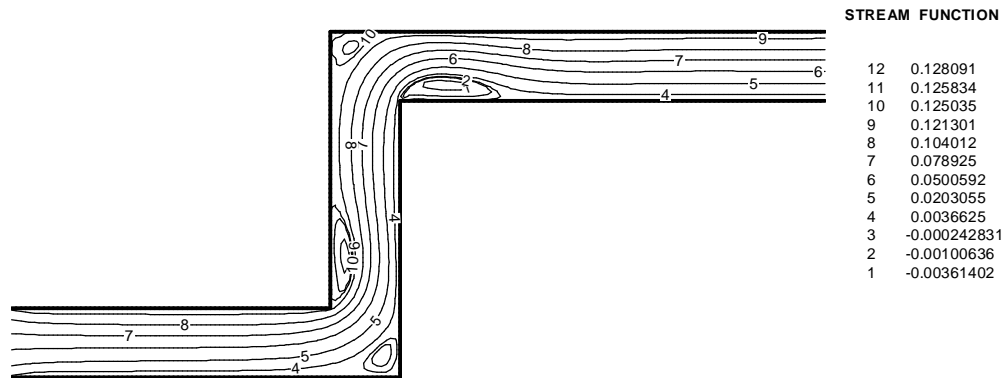
Figure (6) Comparison of the local Nusselt number distribution along the upper duct wall (a) ABCD and lower duct wall (b) EFGH for laminar flow between present prediction and experimental [6], for $H/W=3$ and $Re=300$.



(a) $H/W=2$, $U_{in}=0.5\text{m/s}$, $T_o=40^\circ\text{C}$

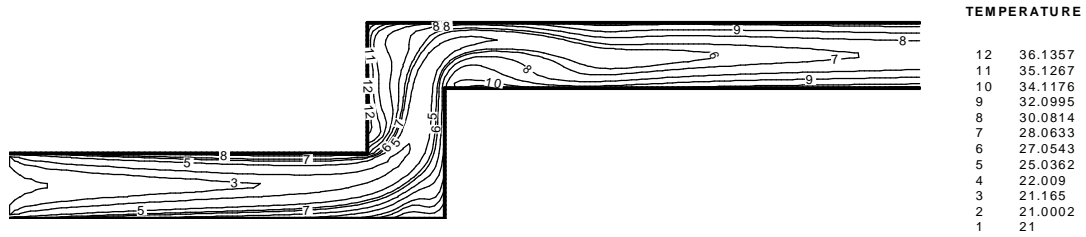


(b) $H/W=3$, $U_{in}=0.5\text{m/s}$, $T_o=40^\circ\text{C}$

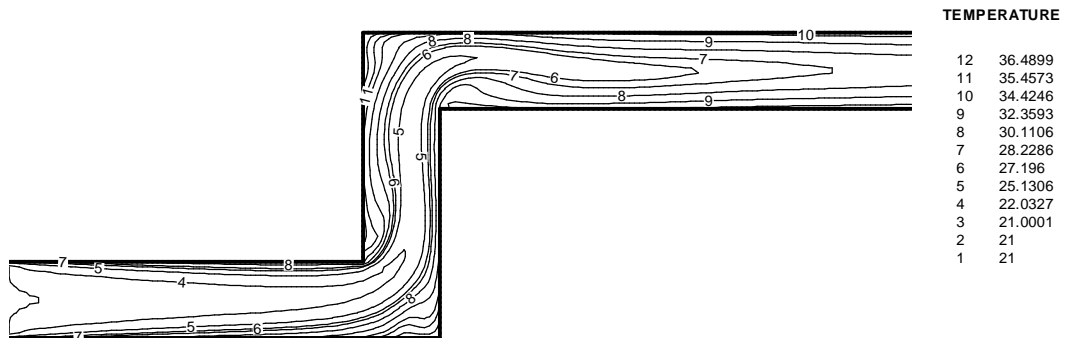


(c) $H/W=4$, $U_{in}=0.5\text{m/s}$, $T_o=40^\circ\text{C}$

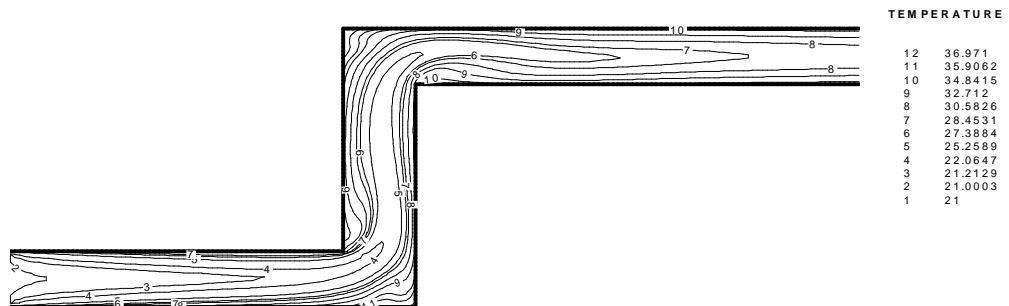
Figure 7 Effect of step ratios on the stream function for turbulent flow, (a- $H/W=2$, b- $H/W=3$, and c- $H/W=4$), $U_{in}=0.5\text{m/s}$, and for heat conducted wall boundary.



a) $H/W=2$, $U_{in}=0.5$ m/s, $T_o=40^\circ\text{C}$



(b) $H/W=3$, $U_{in}=0.5$ m/s, $T_o=40^\circ\text{C}$



(c) $H/W=4$, $U_{in}=0.5$ m/s, $T_o=40^\circ\text{C}$

Figure 8 Contours of temperature distribution for turbulent flow, heat conducted at wall boundary, (a- $H/W=2$, b- $H/W=3$, and c- $H/W=4$), $T_o=40^\circ\text{C}$, and $U_{in}=0.5$ m/s.

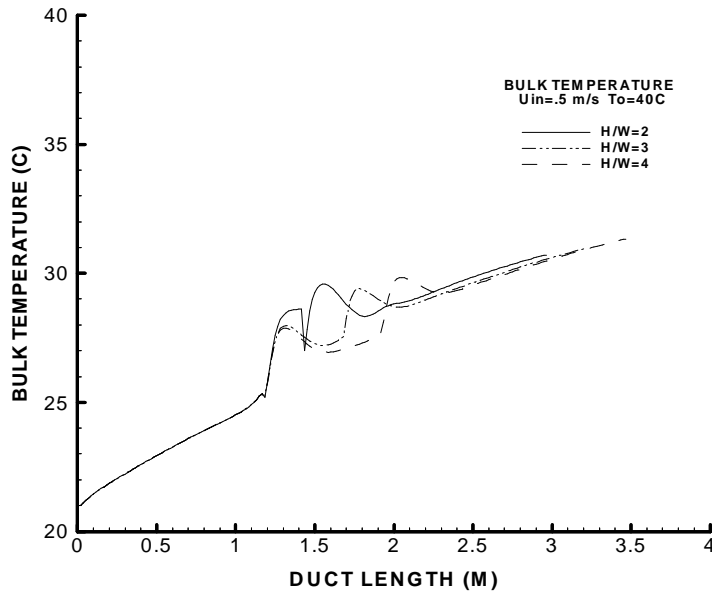


Figure 9 Variation in air bulk temperature along the Fe- duct for turbulent flow, $U_{in}=0.5\text{m/s}$, $T_o= 40 \text{ C}$, and $(H/W=2, 3, \text{ and } 4)$.

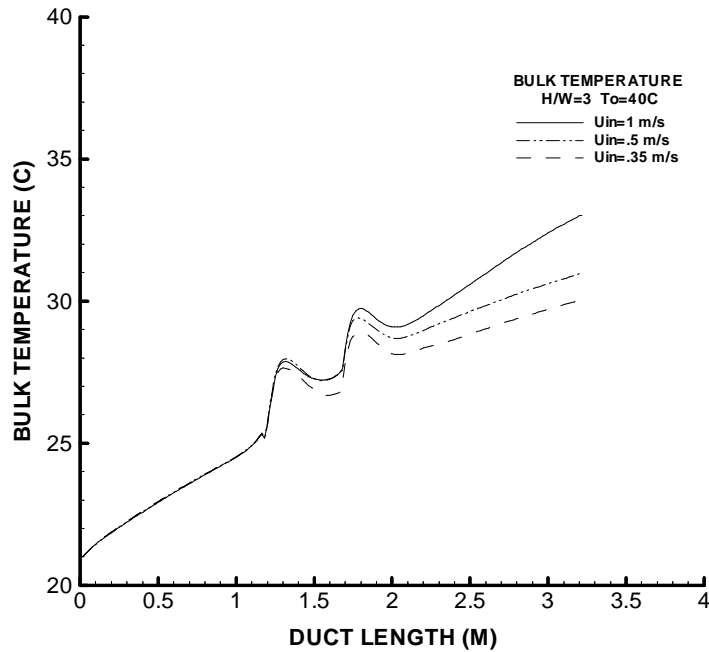
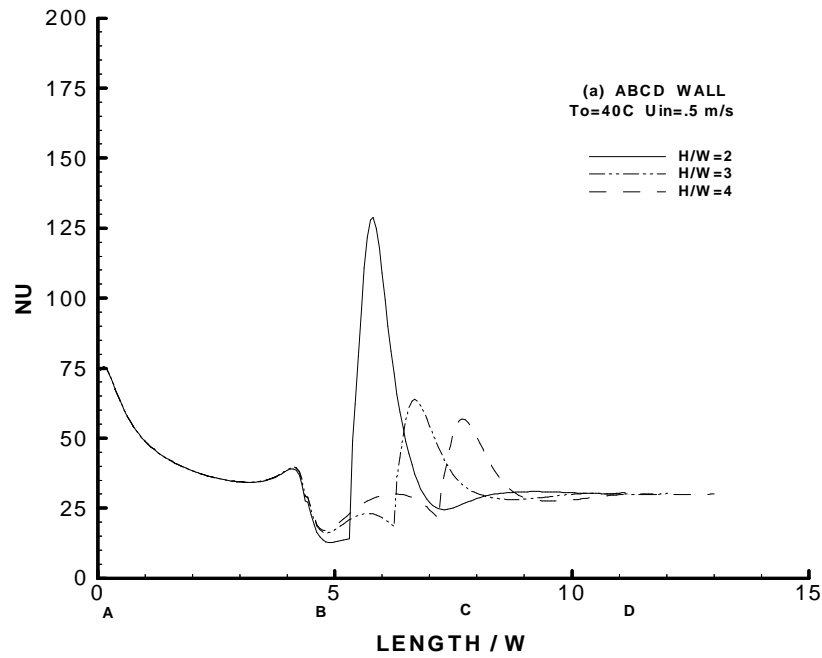
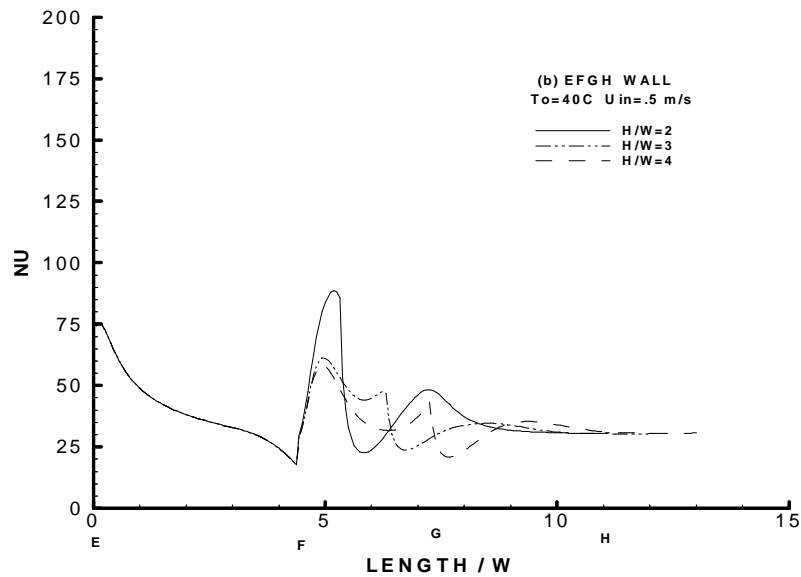


Figure 10 Variation in air bulk temperature along the Fe-duct for turbulent flow, $H/W=3$, $T_o=40^\circ\text{C}$, and $(U_{in}=1, 0.5, \text{ and } 0.35\text{m/s})$.

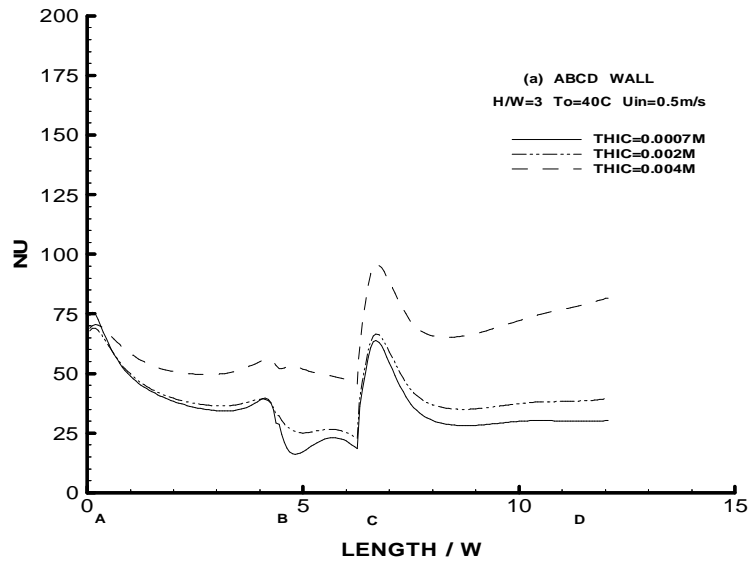


(a)

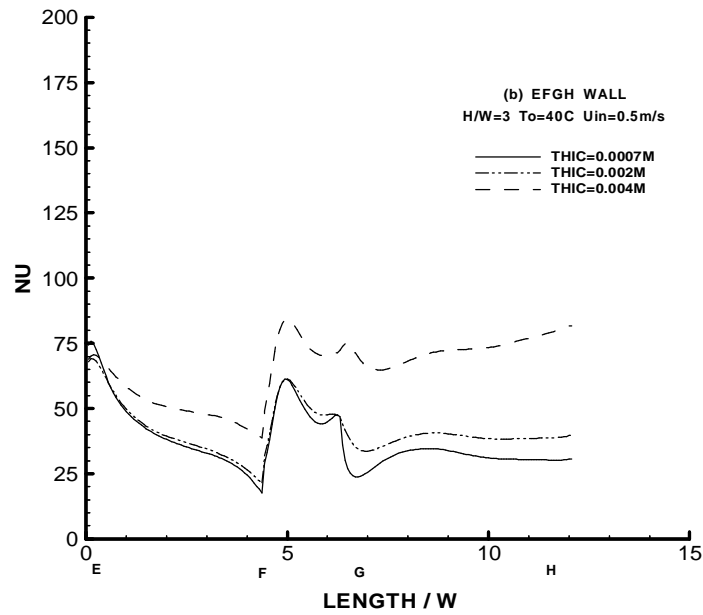


(b)

Figure 11 Local Nusselt number distribution along the upper and lower duct walls, $U_{in}=0.5$ m/s, $T_o=40^{\circ}\text{C}$, and $(H/W=2, 3, \text{ and } 4)$.

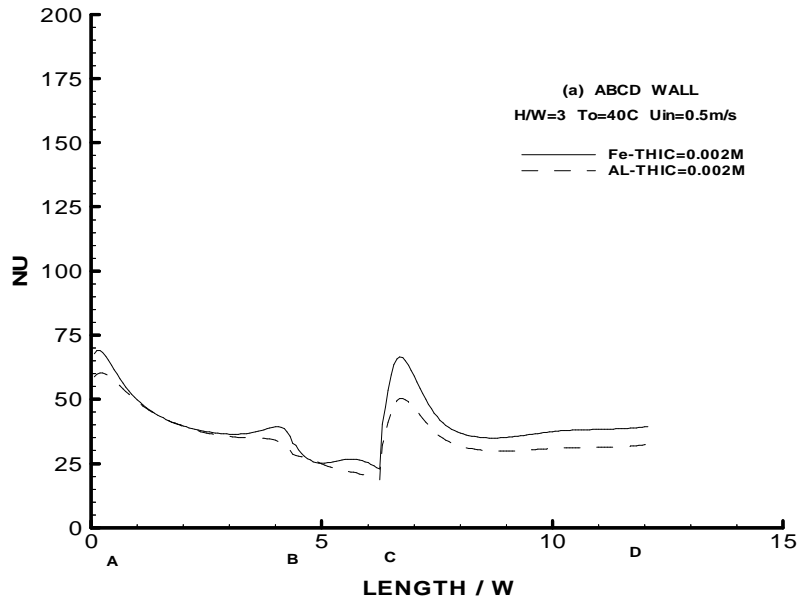


(a)

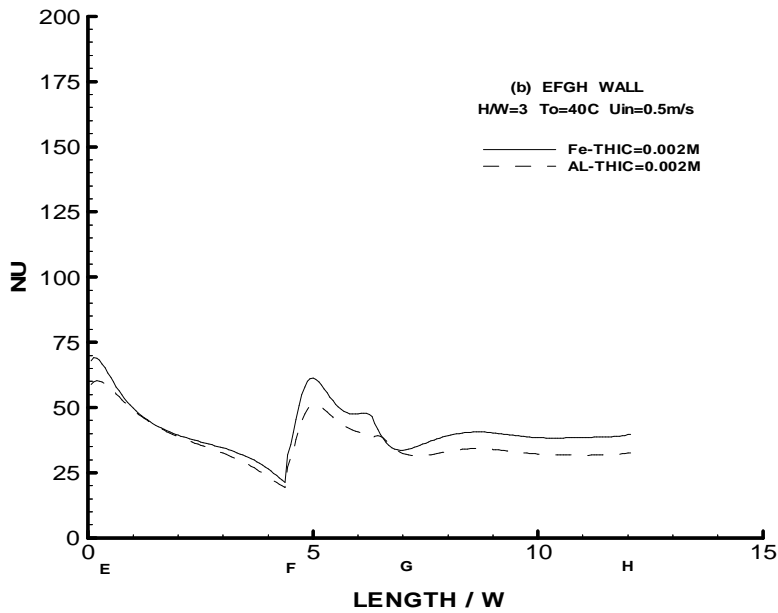


(b)

Figure 12 Local Nusselt number distribution along the upper and lower duct walls for turbulent flow, $H/W=3$, $T_o=40^{\circ}C$, $U_{in}=0.5m/s$, and (Thick=0.0007m, 0.002m, and 0.004m).



(a)



(b)

Figure 13 Local Nusselt number distribution along the upper and lower duct walls for turbulent flow, $H/W=3$, $U_{in}=0.5m/s$, $T_o=40^\circ C$, Thick=0.002m, and (Fe-Metal and Al-Metal).